EFFECTS OF MORPHOLOGY ON ALUMINA STRENGTH AND DUSTINESS

Olsen D., Behrens, C.A., Hamberg, K., Prytz, A.K. and Tveten, E.
Hydro Aluminium Research Centre, Porsgrunn, Norway

Abstract

Hydro Aluminium's recent research on alumina quality has confirmed that fines content and particle strength are the most important of the standard alumina quality parameters related to dustiness. We have also seen significant effects of moisture. However, there are differences in dustiness between alumina from different refineries that cannot be explained by our standard quality parameters. Particle shape and morphology have often been mentioned as candidates to explain these differences. In recent years several methods for quantifying particle morphology have become available. This paper describes breakage tests of alumina in a full size pneumatic transportation rig. Observed breakage is compared to the standard Attrition Index. Material from various stages of the tests has undergone a comprehensive program of Particle Size Distribution analysis, Perra dustiness test, flowability test and morphology analyses. Data on hydrate shows clear relationships between selected morphological characteristics as defined by the Zacknich method and particle strength, while the corresponding picture for calcined alumina is much more blurred. Morphology analyses from different stages of the breakage tests indicate that the degree of weak morphological characteristics is gradually reduced as the breakage proceeds. There are indications that certain morphological characteristics also affect the dustiness as expressed by the Perra index. The number based roundness parameter from the Malvern PharmaVision system also shows clear correlation with dustiness.

1. Introduction

Norsk Hydro's R&D on alumina quality has identified fines content, particle strength and moisture as the main bulk alumina parameters defining alumina dustiness [Olsen, 1999 & 2001]. Operational and meteorological parameters disturb the effects of alumina quality, but it is also clear that alumina related factors not measured by the standard alumina quality parameters have strong influence on alumina dustiness. We have called these "source related effects", because we have not been able to relate them to anything else than the producing refinery. Particle shape, morphology and breakage pattern have been strong candidates for explaining these differences. In recent years suitable and reliable methods of describing and quantifying hydrate and alumina morphology have become available, most notably Charge Contrast Imaging (CCI) for internal morphology and the Zacknich method for external morphology characterisation. We have utilised these techniques to try to explain observed hydrate and alumina particle strength and alumina dustiness, and to describe the observed breakage in a full size pneumatic transportation testrig. Finally we have compared data from the Zacknich characterisation method with two methods offered by Malvern Instruments.

Parts of this work have been strongly inspired by methods and approaches from the AMIRA P575 project. Due to confidentiality reasons, comparison with data and conclusions from P575 will not be made.

2. Tests and measurements

This paper summarises data from the following subprograms:

- Pneumatic transportation breakage tests of six base samples, and subsequent tests and analyses of these base samples and samples of breakage products after 5 and 15 cycles in the testloop.
- Analyses and tests of hydrate samples corresponding to the base alumina samples for the pneumatic breakage tests.
- Analyses and tests of nine additional alumina samples, equal to the subsequent work on the samples from the pneumatic breakage tests.

In addition to the pneumatic transportation breakage tests described later, the following tests and measurements have been used:

- Particle Size Distribution (PSD) by Rotap sieve (round electroformed), <20µm by laser diffraction (Coulter LS 200) on the <45µm sieve fraction.
- Attrition Index (A.I.) by the standard F&H column, using the Alcan method 1173.
- Number based breakage index by running the standard F&H test for 3 minutes and counting particles on a Coulter Counter Multisizer™3.
- Perra Dustiness Index
- Flowability using an Alcoa type funnel test [Hsieh]
- External morphology analysed by CSIRO Minerals in Perth using the Zacknich method. The method requires a single sieve fraction. We used the 75–106 µm fraction.
- Internal morphology by our in-house interpretation of CCI runs made by Prof. Griffin at the University of Western Australia. Twenty particles, randomly selected by UWA, from each sample were characterised as having Radial, Pseudo-Radial or Mosaic structure, one or multiple nuclei, and the degree of "pop-corn" particles. This categorisation is highly subjective, and we dismissed our attempts on defining the degree of voidage.
- Statistical evaluation was done using the Unscrambler™ software from CAMO, mostly Principal Component Analysis (PCA) and PLS[1] regression.

1. PLS: Partial Least Squares Projection to Latent Structures.

KEY WORDS: alumina, dustiness, strength, morphology

Selected data for all alumina samples are shown in Table 4 in the back of this paper.

3. Hydrate strength

Before running the pneumatic transportation breakage tests described later, we were able to obtain corresponding hydrate samples to some of the alumina samples. A total of six hydrate samples were tested. PLS regression showed that the standard hydrate A.I. could be modelled perfectly by using all the information on external and internal morphology. By gradually reducing the number of parameters, 94% of the variation in A.I. could be modelled by just two parameters, the degree of Single Crystal Protrusions (SCP) from the Zacknich method and the fraction of particles with multiple nuclei from CCI, both positively correlated, at correlation coefficients R=0.96 for the calibration model and R=0.91 for the validation model, see Figure 1 showing predicted versus measured hydrate A.I. SCP alone explains 88% of the variance.

Using the same approach for the number based k_{3min}[2] variable, we found that all the variation in k_{3min} could be explained by just two parameters, the degree of SCP (positive correlation) and the fraction of radial structures found in CCI (negative correlation), with correlation coefficients above 0.99 for both calibration and validation model. SCP alone accounts for 74% of the variance. The observation that particles with radial structure create fewer particles during breakage than mosaic and pseudo-radial structures fits well with the findings of Clerin & Laurent [2001] for alumina.

4. Alumina strength

The Zacknich method for external morphology characterisation was developed for hydrate, but we found it interesting to try it also on alumina. This study involves the expanded set of data described later, including samples from the pneumatic transportation breakage tests. Although the morphology of SGA is determined by the hydrate, we did not find the same strong relationship between morphology and strength for SGA as for hydrate. Differences in technology and operating conditions in calcination are probably important elements in explaining this, but even when running the analysis on samples from one basic calcination technology only, our data could not support any credible model to predict SGA A.I. based on external morphology. However, a few effects shone through in all our trials: Radial Texture was always correlated to lower A.I., while Agglomerated Texture, Loose Agglomeration, Spherical Shape and Large Crystallite Size were all correlated to higher A.I. The two latter may be somewhat surprising, but A.I. is just describing the amount of breakage across the 45 µm border, not the breakage products. It is also remarkable that the degree of SCP does not show much effect on SGA A.I. in our data. We have not enough samples with number based k_{3min} values to run a meaningful analysis of those, but the indications are that crystallite size and SCP have the same type of influence for SGA as observed for hydrate.

5. Pneumatic breakage tests

Questions have been raised as to whether the A.I. test gives a realistic measure of alumina breakage during handling. This was tested in the pneumatic transportation testrig at Postec[3] that was configured to give similar velocities, load rates etc. as a selected transport leg at one of our smelters. Six alumina samples, 1000 kg each, was run 15 times through the loop and samples taken from each loop. A sketch of the rig is shown in Figure 2, and key data given in Table 1.

Table 1 — Key data for the pneumatic transportation breakage tests

Length per loop	140 m
Sending pressure	4 bar
Capacity	Ca 20 t/h
Loading ratio	Ca 12-14
Diameter	3"
Number of bends (one loop)	9

Figure 3 shows the increase in <21µm for all samples through the fifteen cycles. The plot for <42µm is very similar. These curves are based on analyses from Postec. The instrument used is a Helos KF equipped with the Quixel wet module, all from Sympatec GmbH in Germany. All other data, graphs and evaluations are based on our own PSD analyses. Sample N showing most breakage comes from a rotary kiln, while all the others come from stationary calciners of two different technologies.

Figure 4 shows the increase in fines content after 15 cycles plotted against the average A.I. for each sample. There is a good correlation between observed breakage in the pneumatic transportation rig and the A.I., indicating that the standard A.I. is suited for ranking the *amount of breakage* in such transportation systems. However, the A.I. gives no information about the breakage process or products (apart from them being smaller than 45 µm), and our experience is that A.I. is not suited for comparing for instance dustiness potential of products from different refineries, precipitation technologies and particle morphologies.

5.1 *Changes in morphology during breakage*

When comparing the external morphology characteristics of the samples from cycles 0 (start), 5 and 15, there is a tendency that the fractions of characteristics normally regarded as weak are reduced through the breakage process. Examples of this are SCP-Yes, Crystallite Size Fine and Texture Agglomerate. Two alternate processes can explain this, and both are expected to happen simultaneously:

1. Corners (SCPs) etc. are knocked off and the particles are "rounded", reducing SCP and irregular shapes.
2. Particles with weak characteristics disintegrate and fall out of the given sieve range.

The development for Crystallite Size Fine is shown in Figure 5 as an example.

6. Perra Dustiness Index

The Perra Dustiness Index normally correlates reasonably well with <45 µm within the normal SGA range of fines content. Our data on 50 samples from 7 different refineries indicate a linear correlation coefficient R of 0.60 against <45µm. Within each source the R-value is normally well above 0.80 [Olsen, 2001]. The six base samples from the pneumatic transportation tests have an R-value of 0.75. However, when we include the samples after 5 and 15

2. k_{3min} = ln(number of particles after 3 minutes attrition/number of particles at start)/180. This parameter is a slightly modified version of a parameter developed in P575.

3. Postec: Telemark Technological Research and Development Center, Dept POSTEC, (POwder Science and TEChnology).

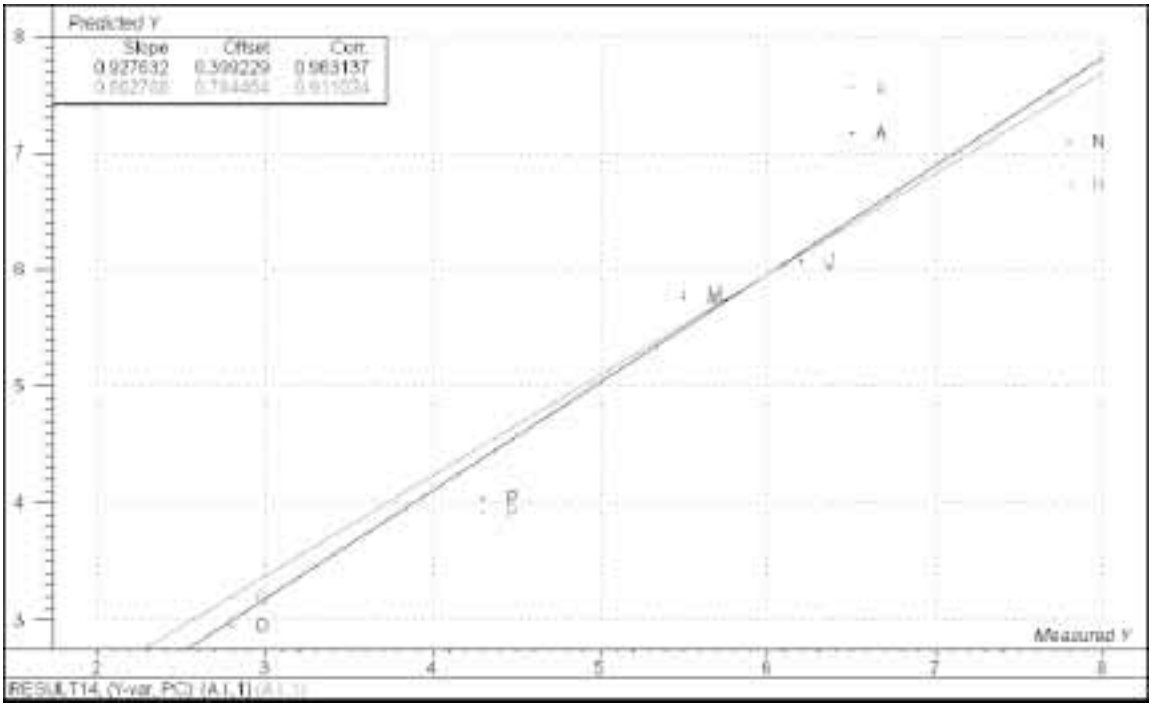

Figure 1 — Predicted hydrate A.I. (y-axis) vs. measured hydrate A.I. (x-axis)

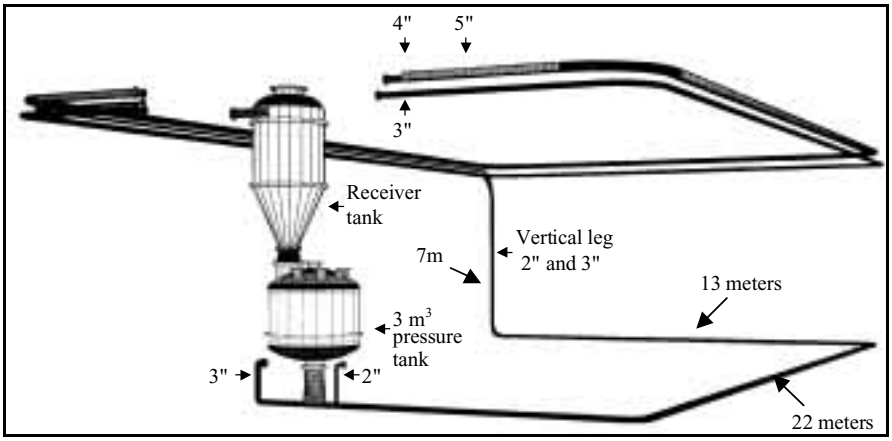

Figure 2 — Sketch of pneumatic transportation testrig at Postec

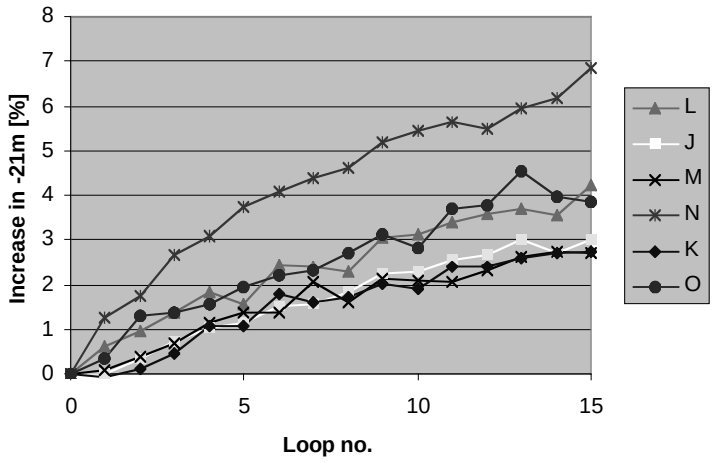

Figure 3 — Increase in fines content during pneumatic transportation breakage tests

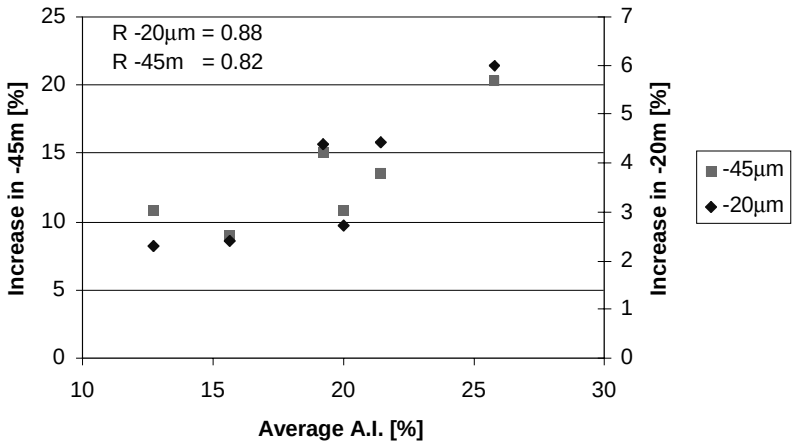

Figure 4 — Increase in fines during pneumatic transportation breakage tests versus A.I.

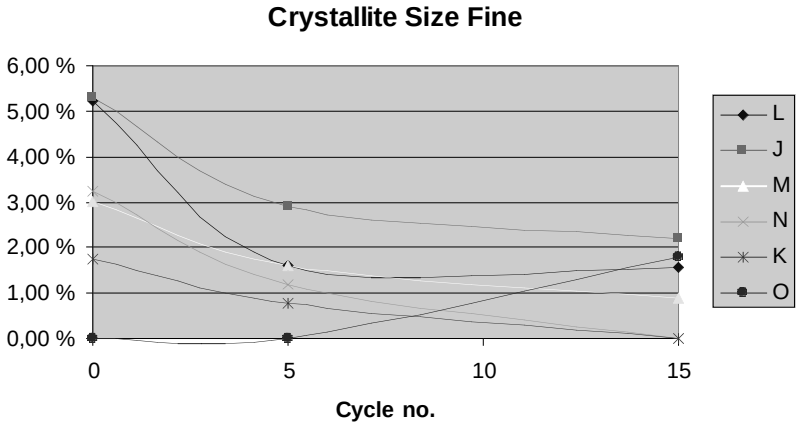

Figure 5 — Changes in Crystallite Size Fine during pneumatic transportation breakage tests

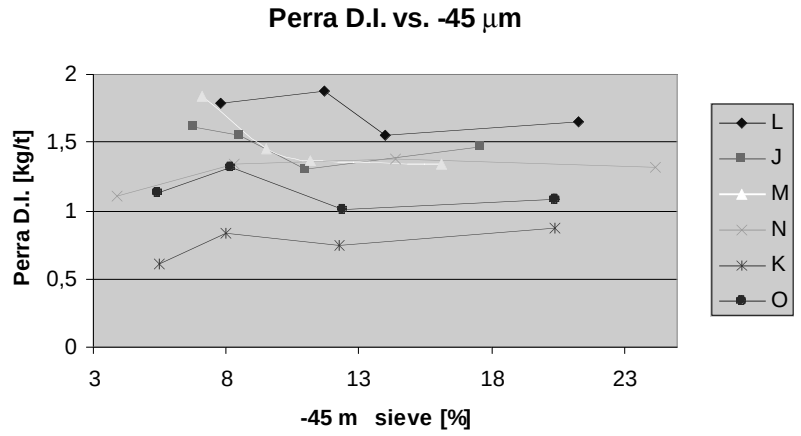

Figure 6 — Perra dustiness index vs. –45 µm during pneumatic transportation breakage tests

cycles, this relationship disappears completely as seen in Figure 6. This levelling off of Perra D.I. at high fines content has also been observed by Authier-Martin [1989] who found a reduction in dustiness index when the –20 µm level exceeded a certain level.

PLS modelling indicated that 77% of the variance in Perra D.I. for the base, 5 and 15 cycles samples for all six sources could be explained by four external morphology parameters and <20 µm with correlation coefficient R=0.86. However, the score plot revealed that the samples could be divided into two distinct populations, see Figure 7. The model did not work within each of these populations, and a simplified model using only <20µm, <45 µm and a population parameter with value 0 for one population and 1 for the other could explain 70% of the variation in Perra D.I. at correlation R=0.78. All the samples from each refinery were located within the same "morphology population". The apparent effect of the morphology parameters could therefore be just a coincident, and there could still be an unknown source related effect behind. There could also be influences from other parameters like for instance flowability. To study this further we decided to expand the dataset in order to try to bridge the gap between the two morphology populations.

6.1 *Expanded dataset*

For the expanded dataset we brought in nine new samples (A through I), covering a wider range of refineries and precipitation technologies and thereby particle morphologies.

A similar PCA of all 27 samples (15 base samples plus 12 samples from cycles 5 and 15 of the pneumatic tests shows that even if the gap has decreased a little, there is still tendencies to a segregation in two populations.

One of our working hypothesis was that when fines content increases above a certain level, the flowability of the material is reduced, resulting in slower flow down the cone of the Perra instrument and thereby reduced energy release and dust generation. The flow funnel tests for the main 11 samples with <45 µm in the 4.5-11.5% range, indicated that the effect of fines were not very strong, although a weak effect of <20 µm was observed. When including the samples from 5 and 15 cycles in the pneumatic transportation tests, with <45 µm levels up to 16%, the effect of fines, especially <20 µm, on flow time became dominant. Most of the 15 cycles samples did not pass through the funnel at all.

Analyses of the PSD of the dust fractions from the Perra instrument showed that 4 of the 11 main samples were much coarser than the others. These samples had 4 of the 5 fastest flow times in the funnel test. Figure 8 below shows the PSD for one of the coarse Perra samples, a typical Perra dust, and a typical dust sample collected above the transportation belt during unloading of an alumina shipment at one of our Norwegian smelters, using a so-called Sochslet nozzle. We see that even normal Perra dust is much coarser than “real” alumina dust, and the even coarser dust caused by too fast flow makes the collected dust from the Perra instrument even less representative.

Somewhat surprisingly, none of the statistical analyses of our data showed any effect of flowability on Perra D.I. worth mentioning.

Results of PLS modelling of Perra D.I. versus various parameters, using a maximum of 4 Principal Components, are given in Table 2. Fines content alone can obviously not be used for predicting the dustiness (Model 1). Introducing mean particle size improves the correlation, but it is still rather weak (Model 2). Adding all the Zacknich morphology parameters (Model 3) increases the correlation coefficient to around 0.7 with 78% explanation of the variance in Perra D.I. Through a trial and error process of gradually removing parameters, it was found that a simplified model using only three of the four Zacknich shape classifiers, <45 µm and mean size (Model 4) was almost as good as the full model (Model 3). Running the same modelling only on the “left population” in the score plot gives almost the same correlation and degree of explanation for the calibration model, but a poorer validation both because of reduced span in the variables and fewer samples. However, this shows that we are not just talking about the difference between two populations, the relationships are also valid within the main population.

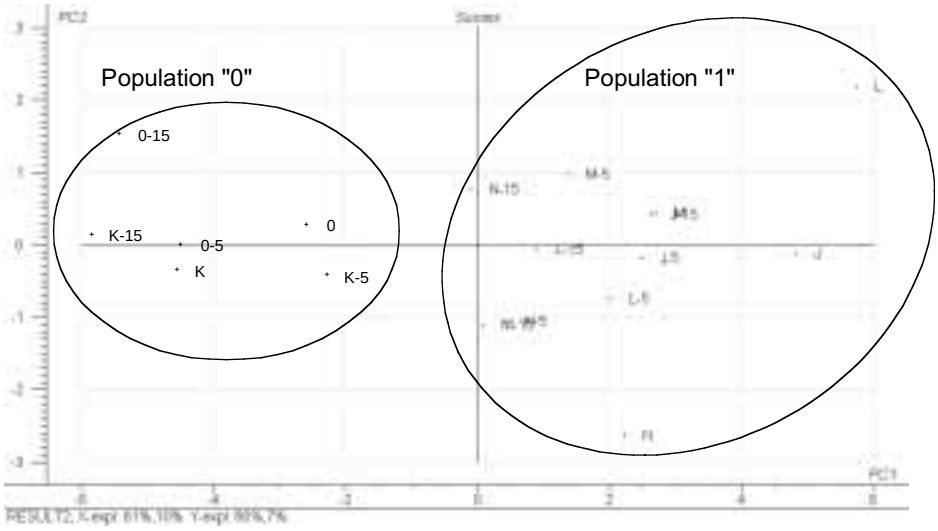

Figure 7 — PCA Score plot showing two populations of samples

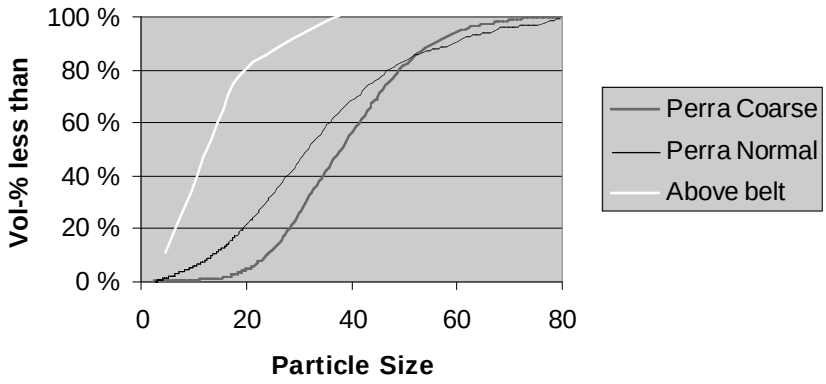

Figure 8 — PSD of Perra dust fraction compared to dust collected above belt during unloading

The loadings plot for the two first components in Model 4 using all 27 samples is shown in Figure 9 below. We see that Irregular and Oblong2 shape and Loose agglomeration are positively correlated with Perra D.I., while the mean particle size in the opposite corner is negatively correlated. Fines content (<45 µm) is also positively correlated with dustiness, but does not have much weight in this set of data. Shape Oblong1 has a weak negative influence in the second component (which accounts for only 4% of the variance).

7. Other methods for morphology characterisation

The 11 "main" samples were also analysed by Malvern Instruments in Malvern, UK using the Sysmex FPIA-2100 instrument (75-106 µm sieve fraction) and the PharmaVision 830 Video Analysis System (whole sample). Initial Principal Component Analyses indicated weak positive correlation between the Shape Spherical parameter from the Zacknich method with the volume based Roundness parameter from the PharmaVision system, and also between the Shape Spherical parameter and the Mean Diameter from the Sysmex. However, a closer look revealed that these relationships were depending totally on 2-3 samples, and when removing these, the apparent correlations disappeared. Based on our limited data, we cannot — at least yet — claim any relationship between the Zacknich morphology parameters and the shape parameters from the two Malvern systems.

It should also be stated that the Zacknich method is a much more comprehensive method developed especially for aluminium trihydrate and yielding much more detailed and specific information. The two Malvern methods are simpler, instrumental methods with different purposes than the Zacknich method.

8. Correlation between Perra D.I. and Malvern number based roundness parameter

We observed a correlation between the number based Roundness parameter from the PharmaVision data and the Perra D.I. with R=0.84. Since this parameter is weighted on numbers, the shape of the smallest particles becomes dominant compared to the volume based Roundness parameter. The correlation indicates that small round particles are dustier than irregular small particles. Table 3 summarises the different models run on the 11 main samples where the Malvern roundness data is available. We see clearly that adding the number based Roundness improves correlation, explained variance and estimation error. RMSEC around 0.12-0.16 is in the same range as the standard deviation for the Perra test.

Table 2 — Summary of PLS regression on all 27 alumina samples

Model ID	Samples (number)	Variables	$R_{calibration}$	$R_{validation}$	Explained variance	RMSEC[4]
1	All (27)	<20 µm, <45 µm	0.15	–0.38	2%	0.300
2	All (27)	<20 µm, <45µm, mean size	0.52	0.38	33%	0.260
3	All (27)	All morph, <45µm, mean size	0.71	0.67	78%	0.214
4	All (27)	Oblong1, Oblong2, Irregular, Loose, Mean, <45 µm	0.72	0.63	60%	0.209
4	Only samples from "left population" (14)	Oblong1, Oblong2, Irregular, Loose, Mean, <45 µm	0.69	0.16	60%	0.173

[4] RMSEC, Root Mean Squared Error on Calibration model.

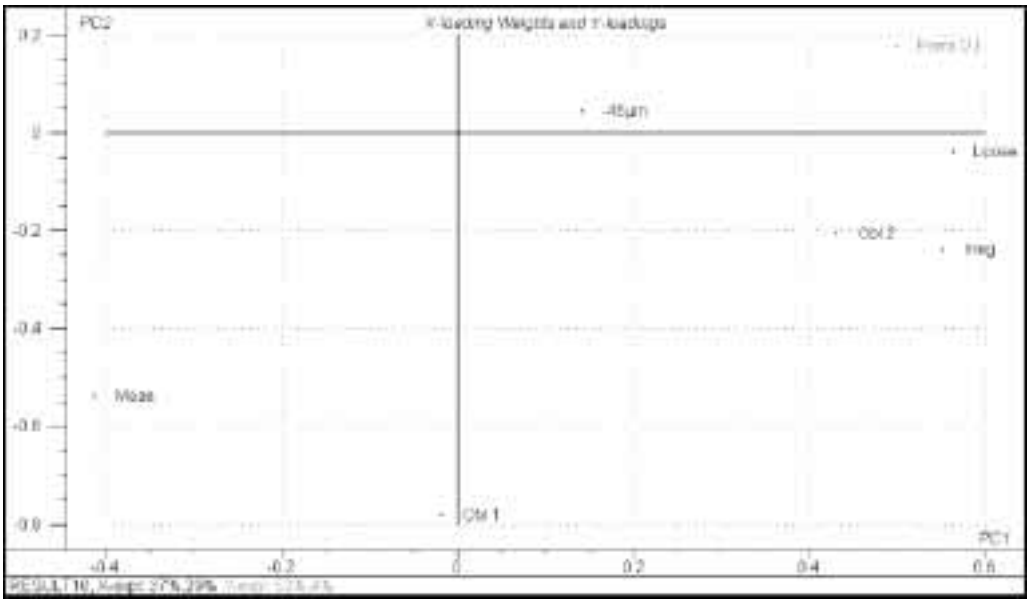

Figure 9 — Loadings plot showing the weight of the parameters on the two first Principal Components

Table 3

Model ID	Samples (number)	Variables	$R_{calibration}$	$R_{validation}$	Explained variance	RMSEC
1	Main (11)	<20 µm, <45 µm	0.69	0.42	47%	0.211
2	Main (11)	<20 µm, <45µm, mean size	0.75	0.40	56%	0.192
3	Main (11)	All morph, <45µm, mean size	0.85	0.48	88%	0.152
4	Main (11)	Oblong1, Oblong2, Irregular, Loose, Mean, <45 µm	0.85	0.57	91%	0.152
4	Only samples from "left population" (9)	Oblong1, Oblong2, Irregular, Loose, Mean, <45 µm	0.79	0.49	94%	0.163
5	Main (11)	RoundNumb	0.84	0.70	71%	0.156
6	Main (11)	RoundNumb, <45 µm and Mean	0.85	0.54	72%	0.152
7	Main (11)	Oblong1, Oblong2, Irregular, Loose, Mean, <45 µm and RoundNumb	0.90	0.84	91%	0.125
7	Only samples from "left population" (9)	Oblong1, Oblong2, Irregular, Loose, Mean, <45 µm and RoundNumb	0.86	0.65	96%	0.135

9. Discussion

Several of the Zacknich morphology parameters are strongly internally correlated. It may be a little incidental which of these correlated parameters are removed during an elimination process. However, when discussing alumina dustiness it seems sensible and intuitively right to end up with shape related parameters.

It may seem contradictory that irregular shape of the larger particles contributes to increased dustiness while deviation from roundness of the smallest particles contributes to reduced dustiness. Our hypothesis for the dusting mechanism is that the dusting potential of a given powder is represented by the amount of dust (fines) present in the material. Inter particular forces tend to moderate the ability to form dust (expressed as mass of dust per unit mass of bulk material). Thus the stronger the inter-particular forces, the more energy is required to create a certain level of dustiness. In order to create dust, the energy involved in the dusting action need to create a fluid dynamic shear field expressing sufficient stress on an agglomerate in order to separate the particles. This hypothesis will be in line (analogy) with the theory of dispersing oil in water where the oil droplet size distribution is determined by a balance between surface tension forces and shear forces created by the mixing action [Drew et.al.]

As soon as the particles or aggregates are dispersed in air away from the dispersing energy source, their behaviour will depend on their terminal settling velocity and air velocity profile in the surrounding environment. In view of the above hypothesis, a few possible explanations for the observed reduced dustiness with increased irregularity of the smallest particles can be proposed:

1. The smallest particles are crystallites with crystal planes that may align with crystal planes on other particles, thus forming aggregates. Inter-particular forces (electrostatic or Van der Waal forces) keep them together. Increasing crystal plane surface per unit mass of particle would correlate with increasing deviation from roundness. Thus, the greater the deviation from roundness, the greater the probability of finding a relatively large surface for attachment to other particles faces.
2. Another possibility is physical friction caused by crystallite edges and corners. The small particles may stick to much larger particles and "hide" in corners or crevices. The more irregular these smaller particles are the more shear force is required to separate them from the bigger ones and the less dusting properties will the powder exhibit.

As the amount of fines in alumina increases, it will tend to loose its free flowing properties and start behave like a cohesive powder. This is explained by the increasing number of particle to particle contact points per unit volume of powder as the amount of fines increases [Enstad]

10. Conclusions

Hydrate morphology as described by the Zacknich method and Charge Contrast Imaging can be used to predict hydrate particle strength; both defined by the standard A.I. and a number based attrition measure. The relation between morphology and strength is not as clear for alumina as for hydrate. This can probably at least partly be explained by differences in calcination operating conditions and technology.

Breakage tests of several alumina samples in a full size pneumatic transportation testrig showed that the observed amount of breakage is well correlated with the standard A.I. There is a slight reduction in the degree of morphological characteristics regarded as weak during the breakage tests indicating that corners (SCPs) etc. are knocked off and the particles are "rounded", reducing SCP and irregular shapes and/or that particles with these weak characteristics disintegrate and fall out of the given sieve range.

Alumina dustiness as defined by the Perra D.I. increases with increasing fines content up to a certain level, an observation that corresponds with Authier-Martin [1989]. Hydro's alumina quality R&D has shown that there are differences in dustiness between alumina sources that cannot be explained by the Particle Size Distribution. Introducing the Zacknich morphology parameters for the alumina greatly improves the prediction of the Perra D.I. The degree of irregular shapes and loose agglomeration seem to be of special importance.

The number based roundness parameter from the Malvern PharmaVision analyses is negatively correlated with the Perra D.I. and improves the model based on fines content, mean particle size and Zacknich shape and agglomeration parameters considerably. It is suggested that this effect of the shape of the smallest particles is related to inter-particular forces.

Acknowledgements

The authors want to thank the following contributors:

- Dean Ilievski and the AMIRA P575 project team at CSIRO Minerals for inspiration and external morphology characterisation.
- Prof. Brendan Griffin at UWA for performing CCI
- Postec for pneumatic breakage tests and other input
- Malvern Instruments and their Norwegian representative Geir Hansen in Malvern Instruments Nordic AB for running Sysmex and PharmaVision analyses.
- Various refineries for providing samples (no one mentioned, no one revealed).

References

Authier-Martin, M. Alumina Handling Dustiness, TMS Light Metals 1989, 103–11.

Clerin, P. and Laurent, V. Alumina particle breakage in attrition test, Light Metals 2001, 41–47.

Drew, T.B. et al. Advances in Chemical Engineering. Vol. 9, Academic Press, 1970.

Enstad, G. Personal communication with C. Behrens 2002–05–16 with reference to H. Rumpf, Chemie-Ing.-Techn. 43, 538/40 (1970).

Hsieh, H.P., Measurement of Flowability and Dustiness of Alumina, Light Metals 1987 (1987) 139–149.

Olsen, D. Alumina dustiness related to physical quality parameters — User experience and R&D in Hydro Aluminium, Fifth International Alumina Quality Workshop, Bunbury, 1999, 1–11.

Olsen, D. Internal Norsk Hydro report, 2001, HRE doc.no 01B_EP8.

Zacknich, A. Characterization of aluminium hydroxide particles from the Bayer process using Neural network and Bayesian classifiers, IEEE Transactions on Neural Networks, 8(4), 919–931.

Table 4 — Selected data for all alumina samples

	Zacknich external morphology parameters											Particle size						
	Shape			SCP	Texture			Size of crystallites			Agglom.	Fines content						
Sample ID	Obl 1	Obl 2	Irreg	Yes	Rad	Mos	Agglom	Large	Small	Fine	Loose	<20µm [%]	<45µm [%]	Mean size [µm]	Flowtime [sec]	A.I. [%]	Malvern RoundNo	Perra [kg/l
A	0,354	0,114	0,133	0,259	0,108	0,146	0,171	0,215	0,272	0,025	0,063	0,64	5,4	127,2	340	22,7	0,733	1,34
B	0,165	0,034	0,034	0,091	0,068	0,000	0,028	0,682	0,000	0,006	0,011	0,40	5,6	107,6	264	26,1	0,733	1,19
C	0,294	0,074	0,081	0,169	0,169	0,037	0,074	0,419	0,118	0,007	0,022	1,13	6,9	116,2	304	10,5	0,723	0,98
D	0,351	0,086	0,063	0,218	0,138	0,029	0,029	0,466	0,109	0,017	0,017	1,17	6,8	115,1	314	11,6	0,743	1,41
E	0,202	0,058	0,019	0,173	0,048	0,010	0,010	0,490	0,038	0,000	0,000	0,92	6,3	131,7	313	19,2	0,733	1,16
F	0,135	0,036	0,036	0,073	0,073	0,010	0,026	0,693	0,010	0,016	0,005	0,79	11,5	104,9	282	29,7	0,762	1,46
G	0,353	0,096	0,059	0,265	0,051	0,029	0,051	0,471	0,044	0,000	0,000	0,47	4,5	121,6	304	22,2	0,732	0,8
H	0,261	0,091	0,102	0,170	0,182	0,000	0,045	0,341	0,057	0,011	0,045	1,00	7,3	129,4	289	20,1	0,732	1,31
I	0,375	0,035	0,035	0,097	0,125	0,000	0,021	0,535	0,028	0,000	0,000	0,71	4,9	129,6	306	17,1	0,724	0,95
J	0,282	0,188	0,123	0,358	0,036	0,139	0,164	0,359	0,214	0,053	0,045	1,68	6,8	117,5	320	21	0,748	1,61
J-5	0,348	0,092	0,130	0,318	0,040	0,099	0,134	0,422	0,141	0,029	0,023	2,64	11	111,1	568	21,1		1,3
J-15	0,358	0,062	0,076	0,307	0,075	0,094	0,115	0,294	0,252	0,022	0,045	4,38	17,6	101,7		18,6		1,46
K	0,311	0,037	0,032	0,094	0,108	0,000	0,020	0,615	0,033	0,018	0,000	0,68	5,5	137,4	324	12,2	0,705	0,61
K-5	0,338	0,029	0,036	0,121	0,039	0,021	0,064	0,486	0,101	0,008	0,008	3,21	12,3	124,6	411	12,3		0,75
K-15	0,262	0,036	0,027	0,051	0,086	0,000	0,009	0,758	0,009	0,000	0,000	5,43	20,4	113,6		13,7		0,87
L	0,234	0,063	0,155	0,352	0,010	0,208	0,179	0,361	0,342	0,052	0,054	1,78	7,8	116,8		22,9		1,79
L-5	0,410	0,089	0,076	0,297	0,022	0,049	0,136	0,405	0,209	0,016	0,054	3,38	14	107,4	444	21,7		1,55
L-15	0,284	0,096	0,100	0,263	0,092	0,072	0,081	0,301	0,176	0,016	0,025	6,20	21,3	97,4		18,6		1,65
M	0,362	0,112	0,061	0,344	0,022	0,140	0,079	0,350	0,261	0,030	0,028	1,70	7,1	121,3		17,3		1,84
M-5	0,240	0,105	0,081	0,331	0,046	0,132	0,081	0,341	0,208	0,016	0,009	2,78	11,2	114,0	513	15,2		1,37
M-15	0,356	0,056	0,126	0,264	0,046	0,035	0,102	0,527	0,137	0,009	0,015	4,12	16,1	106,5	762	13,8		1,34
N	0,360	0,158	0,083	0,371	0,040	0,090	0,086	0,392	0,150	0,032	0,043	0,34	3,9	126,6		28,7		1,1
N-5	0,319	0,078	0,093	0,308	0,090	0,045	0,045	0,309	0,079	0,012	0,046	3,57	14,4	110,4	486	25,3		1,38
N-15	0,303	0,076	0,076	0,333	0,086	0,062	0,091	0,460	0,155	0,000	0,000	6,34	24,2	96,7		22,7		1,32
O	0,348	0,054	0,038	0,127	0,065	0,045	0,024	0,446	0,128	0,000	0,000	1,05	5,4	128,7		18,9		1,13
O-5	0,250	0,022	0,021	0,137	0,091	0,000	0,039	0,581	0,009	0,000	0,009	3,21	12,4	116,1	577	19		1,01
O-15	0,184	0,031	0,026	0,048	0,040	0,000	0,007	0,730	0,013	0,018	0,000	5,43	20,4	103,0		18,3		1,08